

Long- and short-distance contributions to kaon decays

G. Eilam* and M. D. Scadron

Physics Department, University of Arizona, Tucson, Arizona 85721

(Received 10 November 1983)

We work out in detail both the long- and short-distance graphs for $K_{L\gamma\gamma}$, $K_{L\mu\bar{\mu}}$, $K_{\pi e\bar{e}}$, and $K_{\pi\pi\gamma}$ decays. The long-distance amplitudes, which we find to dominate, are related to the $\Delta I = \frac{1}{2}$ enhancement in $K_{2\pi}$ and $K_{3\pi}$ decays. The short-distance diagrams contribute typically about 20%.

MS code no. DL2318 1985 PACS numbers: 13.25.+m, 12.30.-s, 13.40.Hq

I. INTRODUCTION

During the past decade we have witnessed increasing enthusiasm for short-distance quark-model calculations of kaon weak decay processes,¹ perhaps at the expense of the long-distance hadronic pole graphs.^{2,3} However, we now have a better understanding of (i) a possible $\Delta I = \frac{1}{2}$ $K_{2\pi}$ long-distance scale³ [derivable⁴ in the quark model using the Cabibbo-GIM (Glashow-Iliopoulos-Maiani⁵) left-handed quark current], (ii) the η - η' mixing angle⁶ (driven by the quark-annihilation diagram⁷) which enters into many long-distance η and η' weak transitions, (iii) the Kobayashi-Maskawa (KM) weak mixing parameters⁸ (due to the recent measurement of the B -meson lifetime⁹) which enter into all the short distance weak transitions, and (iv) short-distance estimates for heavy quark loops.^{10,11}

In this paper we survey in a *model-independent* manner the following kaon decays and their relation to $\Delta I = \frac{1}{2}$ enhancement: $K \rightarrow \pi\pi$, $K_L \rightarrow \gamma\gamma$, $K_L \rightarrow \mu\bar{\mu}$, $K \rightarrow 3\pi$, $K \rightarrow \pi e\bar{e}$, $K \rightarrow \pi\pi\gamma$ (abbreviated by $K_{2\pi}, \dots$). We find that the $\Delta I = \frac{1}{2}$ long-distance scale of $\langle \pi | H_w | K \rangle$, which accounts for almost all of $K_{2\pi}$, $K_{3\pi}$, and $K_{\pi\pi\gamma}$ (except for $\sim 5\%$ spectator graphs), also contributes to $\sim 120\%$ of the $K_{L\gamma\gamma}$, $K_{L\mu\bar{\mu}}$, and $K_{\pi e\bar{e}}$ amplitudes. We furthermore show that the short-distance $K_{L\gamma\gamma}$ and $K_{L\mu\bar{\mu}}$ boxes and $s \rightarrow d\gamma$ transition in $K_{\pi e\bar{e}}$ are all about 20% of the observed amplitude magnitudes. Since the relative signs between the long- and short-distance $K_{L\gamma\gamma}$ and $K_{\pi e\bar{e}}$ amplitudes can be demonstrated as negative, we suggest that there now exists one universal picture of $\Delta I = \frac{1}{2}$ enhancement which correctly predicts almost all kaon decays. The $K_{S'\pi e\bar{e}}$ and $K_{\pi\nu\bar{\nu}}$ amplitudes are unique in that they receive only short-distance contributions. In a related work,¹² we shall extend this long- and short-distance analysis to the K_L - K_S mass difference.

First, in Sec. II we briefly review the $\Delta I = \frac{1}{2}$ enhancement of $K_{2\pi}$ decays, stressing that any PCAC (partial conservation of axial-vector current) model properly accounting for the momentum variation of the matrix element consistently sets the scale for $\langle \pi | H_w | K \rangle$. The long-distance $K_{3\pi}$ K and π pole graphs also lead to the same magnitude of $\langle \pi | H_w | K \rangle$. Then in Sec. III we investigate in detail the other two-body decays, $K_{L\gamma\gamma}$ and $K_{L\mu\bar{\mu}}$, whose rates are likewise determined by the $\Delta I = \frac{1}{2}$

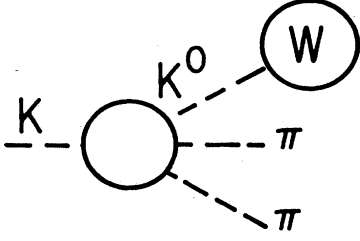
scale $\langle \pi | H_w | K \rangle$. Recent quark-model analyses of the η, η' mixing mechanism^{6,7} have reinforced our approximate belief in the quadratic mass formula, leading to an almost exact cancellation between the long-distance η and η' pole contributions to the $K_{L\gamma\gamma}$ and $K_{L\mu\bar{\mu}}$ amplitudes, leaving the π^0 pole to control both decays. The associated short-distance box graphs as calculated by Refs. 10 and 13 in these two cases are both of order 20%. For $K_{L\gamma\gamma}$, the relative sign between the long- and short-distance amplitudes is then shown to be negative, leading to good agreement between theory and experiment. The observed error on the $\eta_{\mu\bar{\mu}}$ decay rate blurs the conclusion on the $K_{L\mu\bar{\mu}}$ analysis at the 25% level, but still theory and experiment are in rough agreement.

Next in Sec. IV we examine the three-body kaon decays. The four $\Delta I = \frac{1}{2}$ $K_{3\pi}$ decays are linked to $K_{2\pi}$ via current algebra and PCAC¹⁴ and therefore again to the same long-distance scale of $\langle \pi | H_w | K \rangle$. The long-distance $K_{\pi e\bar{e}}^+$ amplitude is also scaled to $\langle \pi | H_w | K \rangle$ by inner-bremsstrahlung diagrams² and, although ambiguous up to a factor of 2 due to the uncertainty regarding the difference of K^+ and π^+ charge radii, it is significantly larger than the short-distance $s \rightarrow d\gamma$ contribution. The latter we calculate, following Refs. 10, 11, and 15, to be roughly 20% of the observed $K_{\pi e\bar{e}}$ amplitude. Again we show that the relative sign between these contributions is negative, making the net theoretical amplitude roughly compatible with experiment. Lastly, we briefly look at $K_{\pi\pi\gamma}$ decay and appeal to the results of Ref. 16, where it is shown that the inner-bremsstrahlung graphs approximately match the observed $K_S \rightarrow \pi^+\pi^-\gamma$ and $K^+ \rightarrow \pi^+\pi^0\gamma$ branching ratios. We argue that the former is scaled to $K_S \rightarrow \pi^+\pi^-$ and therefore to the $\Delta I = \frac{1}{2}$ -dominated long-distance scale of $\langle \pi | H_w | K \rangle$. Finally, in Sec. V, we summarize these results, stressing that *all* kaon weak decays (except K_{12} and $K_{\pi\pi}^+$) stem from the same $\Delta I = \frac{1}{2}$ scale of $\langle \pi | H_w | K \rangle$.

II. $K_{2\pi,3\pi}$ PCAC SCALE

We remind the reader that PCAC applied naively to a soft π^0 in $K_{2\pi^0}$ decay or a π^+ or π^- in $K_{\pi^+\pi^-}$ decay leads to different (unphysical) $\Delta I = \frac{1}{2}$ amplitudes even though isospin symmetry dictates that

$$\langle \pi^+\pi^- | H_w | K^0 \rangle = \langle \pi^0\pi^0 | H_w | K^0 \rangle$$

FIG. 1. Long-distance $K_{2\pi}$ kaon tadpole diagram.

for H_w transforming like $\Delta I = \frac{1}{2}$. The problem is in the strong $K\pi$ momentum variation of the model $K_{2\pi}$ "tadpole" amplitude M_P of Fig. 1 (see, e.g., Ref. 3). Accounting for the rapid momentum variation of the Weinberg¹⁷ $K\pi$ amplitude while conserving momentum^{3,4} in

$$M = M_{cc} + M_P - M_P(p \rightarrow 0),$$

or alternatively reformulating the entire problem in terms of a nonlinear chiral $U(3) \times U(3)$ invariant Lagrangian,¹⁸ one is always led to the *same* PCAC on-shell relation:

$$|\langle \pi\pi | H_w | K_S \rangle| = \frac{1}{f_\pi} |\langle \pi^0 | H_w | K_L \rangle|, \quad (1)$$

where $f_\pi \simeq 93$ MeV. The right-hand side of (1) is *twice* the inconsistent naive PCAC result as found in Refs. 2. Given the validity of (1), the observed¹⁹ $K_{2\pi}^0 \Delta I = \frac{1}{2}$ rate requires the scale

$$|\langle \pi^0 | H_w | K_L \rangle| \simeq 3.9 \times 10^{-8} \text{ GeV}^2. \quad (2)$$

For $K_{3\pi}$ decays, however, the PCAC rapidly varying $K\pi$ and $\pi\pi$ pole structure of the K plus π pole graphs of Fig. 2 directly gives the pure $K_{3\pi}$ pole model on-shell relation between $\Delta I = \frac{1}{2}$ amplitudes:

$$|\langle 3\pi^0 | H_w | K_L \rangle| = \frac{1}{2f_\pi^2} |\langle \pi^0 | H_w | K_L \rangle| \quad (3a)$$

for $f_\pi \simeq 93$ MeV, where Figs. 2(a) and 2(b) each contribute equally to (3a). Equation (3a) also follows in the nonlinear-chiral-Lagrangian scheme,¹⁸ and again (3a) is *twice* what one obtains in the naive soft-pion approach of Ref. 2. Fitting (3a) to the observed¹⁹ $K_{3\pi}$ rates with³

$$|\langle 3\pi^0 | H_w | K_L \rangle| \simeq 2.5 \times 10^{-6},$$

one finds

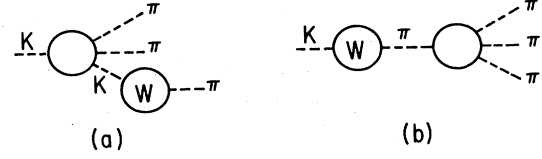
$$|\langle \pi^0 | H_w | K_L \rangle| \simeq 4.3 \times 10^{-8} \text{ GeV}^2. \quad (3b)$$

Since (2) and (3b) are practically identical and well within the expected PCAC errors and slight $\Delta I = \frac{3}{2}$ contamination of (3), we shall henceforth assume the scale (2) when considering other kaon decays in this study.

III. $K_L \rightarrow \gamma\gamma$ and $K_L \rightarrow \mu^+\mu^-$ DECAYS

We now investigate in detail both long- and short-distance contributions to the $K_{L\gamma\gamma}$ decay amplitude, which we write as

$$M_{K_L\gamma\gamma} = M_{K_L\gamma\gamma}^{\text{LD}} + M_{K_L\gamma\gamma}^{\text{SD}}, \quad (4)$$

FIG. 2. Long-distance kaon (a) and pion (b) pole graphs for $K \rightarrow 3\pi$ decay.

where SD stands for short distance (or structure dependent in hadron language). The long-distance (LD) amplitude corresponds to the hadronic π^0 , η , and η' poles of Fig. 3, which give

$$M_{K_L\gamma\gamma}^{\text{LD}} = \frac{\langle \pi^0 | H_w | K_L \rangle}{m_K^2 - m_\pi^2} M_{\pi\gamma\gamma} + \frac{\langle \eta | H_w | K_L \rangle}{m_K^2 - m_\eta^2} M_{\eta\gamma\gamma} + \frac{\langle \eta' | H_w | K_L \rangle}{m_K^2 - m_{\eta'}^2} M_{\eta'\gamma\gamma}, \quad (5)$$

where the weak transitions are of the dominant $\Delta I = \frac{1}{2}$ tadpole form as given by (2). Note that the first π^0 pole term in (5), of magnitude

$$|\langle \pi^0 | H_w | K_L \rangle| (m_K^2 - m_\pi^2)^{-1} \simeq 1.69 \times 10^{-7},$$

is already close to the experimental value¹⁹

$$\left| \frac{M_{K_L\gamma\gamma}}{M_{\pi^0\gamma\gamma}} \right|_{\text{expt}} = \left[\left(\frac{m_\pi}{m_K} \right)^3 \frac{\Gamma_{K_L\gamma\gamma}}{\Gamma_{\pi\gamma\gamma}} \right]^{1/2} = (1.26 \pm 0.10) \times 10^{-7}. \quad (6)$$

To account for the η and η' contributions in (5), it is most transparent to carry out the mixing relative to the $I=0$ nonstrange-strange quark basis,⁷ where the effect of gluon exchanges generates the re-diagonalization,

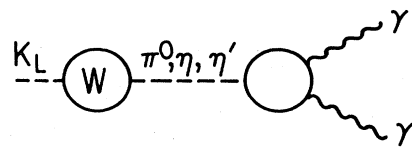
$$|\eta\rangle = \cos\phi |\eta_{\text{NS}}\rangle - \sin\phi |\eta_S\rangle, \quad (7a)$$

$$|\eta'\rangle = \sin\phi |\eta_{\text{NS}}\rangle + \cos\phi |\eta_S\rangle \quad (7b)$$

with the mixing angle found from⁶

$$\tan^2\phi = \frac{(m_{\eta'}^2 - m_S^2)(m_\eta^2 - m_\pi^2)}{(m_\eta^2 - m_\pi^2)(m_S^2 - m_{\eta'}^2)}, \quad \phi \simeq 42.0^\circ \quad (8)$$

for $m_S^2 = 2m_K^2 - m_\pi^2$. Then substituting (8) into (7) we obtain

FIG. 3. Long-distance π^0 , η , η' meson pole graphs for $K_L \rightarrow \gamma\gamma$ decay.

$$\frac{M_{\eta\gamma\gamma}}{M_{\pi\gamma\gamma}} = \frac{1}{3}(5 \cos\phi - \sqrt{2} \sin\phi) \approx 0.923, \quad (9a)$$

$$\frac{M_{\eta'\gamma\gamma}}{M_{\pi\gamma\gamma}} = \frac{1}{3}(5 \sin\phi + \sqrt{2} \cos\phi) \approx 1.466, \quad (9b)$$

and for $\langle P^i | H_w^6 | P^j \rangle$ transforming like d^{i6j} in the U(3) quark model,

$$\frac{\langle \eta | H_w | K_L \rangle}{\langle \pi^0 | H_w | K_L \rangle} = -(\cos\phi - \sqrt{2} \sin\phi) \approx 0.203, \quad (10a)$$

$$\frac{\langle \eta' | H_w | K_L \rangle}{\langle \pi^0 | H_w | K_L \rangle} = -(\sin\phi + \sqrt{2} \cos\phi) \approx -1.720. \quad (10b)$$

We spell out this mixing analysis in detail in order to emphasize the nearly complete cancellation³ of the η and η' pole contributions in (5), leading to

$$\left| \frac{M_{K_L\gamma\gamma}}{M_{\pi\gamma\gamma}} \right|_{\text{LD}} \simeq \frac{|\langle \pi^0 | H_w | K_L \rangle|}{m_K^2 - m_\pi^2} [1 - 0.804 + 0.864] \simeq 1.79 \times 10^{-7}. \quad (11)$$

If we had ignored the η' pole term, then the magnitude of (11) would drop by a factor of 5. However, the above quark-based mixing picture is further supported by the QCD calculation of the U(1) anomaly²⁰ and $\phi \simeq 42^\circ$ corresponds to $\theta = \phi - \tan^{-1}\sqrt{2} \simeq -12.7^\circ$, relative to the singlet-octet basis which is close to the conventional quadratic-mass-formula value of $\theta \simeq -11^\circ$. Thus we shall accept (11) as an accurate estimate of the long-distance hadronic component of the $K_L\gamma\gamma$ amplitude.

In order to include the short-distance “box” graph of Fig. 4, we follow Ma and Pramudita¹³ who estimate that the u -quark graph in Fig. 4 dominates over the c - and t -quark contributions in the KM matrix,^{8,21} giving

$$|M_{K_L\gamma\gamma}|_{\text{SD}} \sim \frac{\sqrt{2}}{\pi} \alpha f_K G_{FS_1} c_1 c_3. \quad (12)$$

Combining (12) with the $\pi^0\gamma\gamma$ anomaly²² $\alpha/\pi f_\pi$ leads to only a 20% correction to (11). The relative sign between Figs. 3 and 4 is *negative* because, while the relative sign is positive between $M_{K_L\gamma\gamma}^{\text{LD}}$ and $M_{\pi\gamma\gamma}$ in (5) for $\langle \pi^0 | H_w | K_L \rangle$ positive²³ as determined in Ref. 4, and likewise for $M_{K_L\gamma\gamma}^{\text{SD}}$ as found in Ref. 13, the KM-matrix convention for s_1 in Ref. 13 (and in Ref. 21) is opposite to that of the GIM current⁵ as used in Ref. 4. Thus we subtract (12) from (11) to obtain the total $K_L\gamma\gamma$ amplitude relative to $\pi^0\gamma\gamma$,

$$\begin{aligned} |M_{K_L\gamma\gamma}/M_{\pi\gamma\gamma}| &\simeq (1.79 - 0.39) \times 10^{-7} \\ &= 1.40 \times 10^{-7}, \end{aligned} \quad (13)$$

very close indeed to the observed ratio (6). In passing, we note that the quark-model choice for the η - η' mixing angle ($\phi = 42.0^\circ$ or $\theta = -12.7^\circ$) uniquely leads to (13). If we instead had taken the quadratic mass formula version ($\theta = -10.7^\circ$, $\phi = 44.0^\circ$), then the long-distance amplitude (11) decreases by $\sim 20\%$, thus spoiling the role of the short-distance amplitude in (13).

Next we turn to $K_{L\mu\bar{\mu}}$ decay, treating the long-distance hadronic π^0 , η , and η' , poles of Fig. 5 in a manner similar to $K_L\gamma\gamma$ decay. The analog of (5) is then (since the weak transitions can be taken as real),

$$\begin{aligned} \text{Re}M_{K_L\mu\bar{\mu}}^{\text{LD}} &= \frac{\langle \pi^0 | H_w | K_L \rangle}{m_K^2 - m_\pi^2} \text{Re}M_{\pi\mu\bar{\mu}} \\ &+ \frac{\langle \eta | H_w | K_L \rangle}{m_K^2 - m_\eta^2} \text{Re}M_{\eta\mu\bar{\mu}} \\ &+ \frac{\langle \eta' | H_w | K_L \rangle}{m_K^2 - m_{\eta'}^2} \text{Re}M_{\eta'\mu\bar{\mu}}. \end{aligned} \quad (14)$$

Just as in the $K_L\gamma\gamma$ case, where we set the off-shell scale to the measured $\pi^0\gamma\gamma$ rate and fixed the $\eta\gamma\gamma$, $\eta'\gamma\gamma$ amplitude by SU(3) and mixing, so here we fix the measured $\eta_{\mu\bar{\mu}}$ rate and determine the off-shell $\pi^0_{\mu\bar{\mu}}$, $\eta_{\mu\bar{\mu}}$ amplitudes via the same mixing procedure. Once again the η and η' pole contributions almost cancel for $\phi \simeq 42^\circ$, leading to the amplitude ratio determined from (14),

$$\begin{aligned} \left| \frac{\text{Re}M_{K_L\mu\bar{\mu}}^{\text{LD}}}{\text{Re}M_{\eta\mu\bar{\mu}}} \right| &\simeq (1.83 - 1.59 + 1.71) \times 10^{-7} \\ &\simeq 1.95 \times 10^{-7}. \end{aligned} \quad (15)$$

To compare (15) with experiment, we must fold in the observed $K_{L\mu\bar{\mu}}$ and $\eta_{\mu\bar{\mu}}$ decay rates with the absorptive parts of the 2γ intermediate states. In particular, one finds²⁴

$$|M_{K_L\mu\bar{\mu}}| = [4\pi\Gamma/p]^{1/2} = (2.5 \pm 0.3) \times 10^{-12}, \quad (16a)$$

$$\begin{aligned} |\text{Im}M_{K_L\mu\bar{\mu}}| &= \frac{\alpha m_\mu}{4} |M_{K_L\gamma\gamma}| \frac{1}{\beta_K} \ln \left[\frac{1 + \beta_K}{1 - \beta_K} \right] \\ &\simeq 2.0 \times 10^{-12}, \end{aligned} \quad (16b)$$

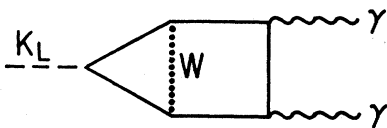


FIG. 4. Short-distance quark box diagram for $K_L \rightarrow \gamma\gamma$ decay.

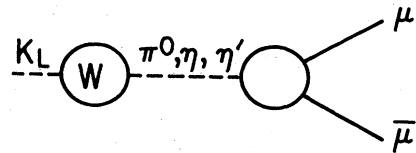


FIG. 5. Long-distance π^0 , η , η' meson pole graphs for $K_L \rightarrow \mu\bar{\mu}$ decay.

for

$$\beta_K^2 = 1 - 4m_\mu^2/m_K^2$$

and then (16) implies

$$|\text{Re}M_{K_L\mu\mu}| = (1.5 \pm 0.2) \times 10^{-12}.$$

Similarly for $\eta_{\mu\bar{\mu}}$ decay, one obtains

$$|\text{Re}M_{\eta\mu\mu}| = (1.0 \pm 0.2) \times 10^{-5}.$$

Dividing one amplitude by the other, we deduce that

$$\left| \frac{\text{Re}M_{K_L\mu\mu}}{\text{Re}M_{\eta\mu\mu}} \right|_{\text{expt}} = (1.6 \pm 0.4) \times 10^{-7}. \quad (17)$$

It is also possible to employ a (quark) model to obtain estimates²⁵ of $\text{Re}M_{\eta\mu\mu}$, but we shall refer only to experiment here.

Finally, one must add the short-distance second-order weak box graph²⁶ of Fig. 6. Following the work of Inami and Lim,¹⁰ Ref. 27 expresses the box-graph contribution (here dominated by the t quark) as

$$|M_{K_L\mu\mu}^{\text{SD}}| \simeq s_1 c_1 s_2^2 \times 10^{-9} G(x_t), \quad (18a)$$

$$G(x_t) = \frac{3}{4} \left[\frac{x_t}{x_t - 1} \right]^2 \ln x_t + \frac{x_t}{4} + \frac{3}{4} \frac{x_t}{1 - x_t}, \quad (18b)$$

where $x_t = m_t^2/m_W^2$. For⁹ $s_3 \sim 0$, $s_2 \sim 0.1$, and $m_t \lesssim 40$ GeV, (18) is of the order of the error on (17). Thus we conclude that the long-distance amplitude (14) and ratio (15) for second-order photon exchange dominates $K_{L\mu\bar{\mu}}$ decay and the ratio (17) over the short-distance second-order weak box graph. Alternatively, Ref. 27 examines the branching ratio $B(K_L \rightarrow \mu\bar{\mu}/\gamma\gamma)$ whose dominant long-distance part is essentially independent of the scale of $\langle \pi | H_w | K \rangle$. The dominance of the LD over the SD part again follows, including perhaps a small (LD) K^* pole component.

IV. THREE-BODY KAON DECAYS

A. $K_{3\pi}$

First we return to the long-distance pole-model graphs of Figs. 2 and Eqs. (3). As is well understood,¹⁴ the direct soft-pion limit of the $K_{3\pi}/K_{2\pi}$ ratio is

$$|M_{K_L 3\pi^0}/M_{K_S 2\pi^0}| \simeq (2f_\pi)^{-1}, \quad (19)$$

which also follows from (1) and (3). While this suggests that Fig. 1 is likewise a long-distance $K_{2\pi}$ pole graph, it is also possible to model $K_{2\pi^0}$ according to a short-distance

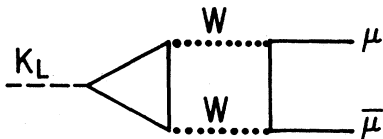


FIG. 6. Short-distance second-order W -exchange box diagram for $K_L \rightarrow \mu\bar{\mu}$ decay.

“penguin” graph,¹ although the latter scale appears to be too small²⁸ to be the origin of the $\Delta I = \frac{1}{2}$ rule. Since we wish to present this analysis in as model-independent a fashion as possible, we shall avoid a long- or short-distance interpretation of $K_{2\pi^0}$ decays but continue to call $\langle \pi | H_w | K \rangle$ and the related meson-pole graphs like Figs. 2, 3, and 5 as “long-distance contributions.”

B. $K_{\pi e\bar{e}}$

The general form of this matrix element is

$$M_{K_{\pi e\bar{e}}} = A (p_K + p_\pi)^\mu \bar{u}_e \gamma_\mu v_{\bar{e}}, \quad (20)$$

where the observed $K^+ \rightarrow \pi^+ e\bar{e}$ rate¹⁹ requires¹⁵

$$|A|_{\text{expt}} = (1.8 \pm 0.2) \times 10^{-9} m_K^{-2}. \quad (21)$$

The associated long-distance “inner-bremsstrahlung” graphs of Fig. 7 correspond to the amplitude

$$|A_{\text{LD}}| = e^2 \frac{|\langle \pi^+ | H_w | K^+ \rangle|}{m_K^2 - m_\pi^2} \left| \frac{F_{\pi^+}(Q^2) - F_{K^+}(Q^2)}{Q^2} \right|, \quad (22)$$

where $Q^2 = (p_K - p_\pi)^2$ is the momentum transfer invariant of the photon and the $\Delta I = \frac{1}{2}$ structure of H_w requires²⁹

$$\langle \pi^+ | H_w | K^+ \rangle = \langle \pi^0 | H_w | K_L \rangle.$$

The latter is the $\Delta I = \frac{1}{2}$ scale given by (2).

Unfortunately, the charge-radii difference in (22) is somewhat ambiguous at the present time,³⁰ with the vector-dominance-model (VDM) value³¹ and the quark-model value³² about one-third the observed difference of charge radii³⁰

$$\begin{aligned} F'_{\pi^+}(0) - F'_{K^+}(0) &\simeq \frac{1}{6} (r_{\pi^+}^2 - r_{K^+}^2) \\ &\simeq \frac{1}{6} (0.48 \text{ fm}^2 - 0.28 \text{ fm}^2) \\ &= (0.21 \pm 0.08) m_K^{-2}. \end{aligned} \quad (23)$$

In (23) we have excluded the one observed low value for $r_{\pi^+}^2$, the remaining values averaging³⁰

$$r_{\pi^+}^2 = (0.48 \pm 0.01) \text{ fm}^2.$$

Combining (23) with (22) and (2), we find

$$|A_{\text{LD}}| = (3.2 \pm 1.3) \times 10^{-9} m_K^{-2}. \quad (24)$$

Since (24) is twice the experimental value (21), whether we adopt (24) or the smaller VDM—quark-model version, the

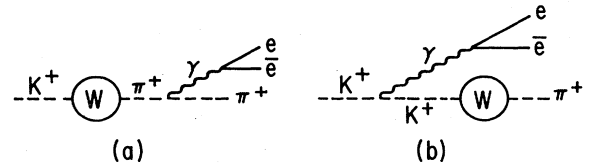


FIG. 7. Long-distance pion (a) and kaon (b) pole inner-bremsstrahlung graphs for $K^+ \rightarrow \pi^+ e\bar{e}$ decay.

long-distance contribution to $K_{\pi e \bar{e}}^+$ certainly cannot be neglected.

As for the short-distance contribution, we follow Ref. 15 and consider only the $\bar{s} \rightarrow \bar{d} \gamma$ quark transitions of Fig.

8 for $K^+ \rightarrow \pi^+ e \bar{e}$ decay. In order to account for the heavy-quark loops in Figs. 8, we again apply the analysis of Refs. 10 and 11, finding from the latter reference the effective $\bar{s} \rightarrow \bar{d} \gamma$ quark current ($e > 0$)

$$j_{\mu,SD}^{\text{eff}} = -\frac{e}{8\pi^2} \frac{G_F}{\sqrt{2}} \left[\sum_{i=u,c,t} V_{is}^* V_{id} F(x_i) \right] Q^2 \bar{s} \gamma_{\mu} d, \quad x_i = m_i^2/m_W^2, \quad (25a)$$

$$F(x) = \frac{1}{1-x} \left[-\frac{23}{108} - \frac{1}{18} \frac{x}{1-x} - \frac{5}{54} x + \frac{2}{3} \frac{x^2}{(1-x)^2} + \frac{2}{9} \frac{x}{(1-x)^2} - \frac{1}{3} \frac{x}{(1-x)^2} \ln x + \frac{2}{9} \frac{x}{(1-x)^3} \ln x + \frac{2}{3} \frac{x^3}{(1-x)^3} \ln x \right. \\ \left. + \frac{1}{2} \frac{x^2}{(1-x)^2} \ln x - \frac{4}{9} \frac{1}{1-x} + \frac{4}{9} \frac{1}{(1-x)^2} + \frac{4}{9} \frac{1}{(1-x)^3} \ln x - \frac{2}{3} \frac{1}{(1-x)^2} \ln x \right]. \quad (25b)$$

In (25a) we have retained only the covariant which contributes to the $K^+ \rightarrow \pi^+$ transition, i.e.,

$$\langle \pi^+ | \bar{s} \gamma_{\mu} d | K^+ \rangle = (p_K + p_{\pi})_{\mu}.$$

Combining Fig. 8 with the photon propagator and $e \bar{e}$ pair, we obtain the form (20) with

$$|A_{SD}| \simeq \frac{\alpha G_F}{2\pi\sqrt{2}} (0.714 s_1 c_1 c_2^2 c_3) \simeq 0.36 \times 10^{-9} m_K^{-2} \quad (26)$$

for $s_3 \ll s_2 \sim 0.1$, practically independent of the top-quark mass.

The relative sign between (22) and (26) is *negative* because the VVF sum in (25a) is negative, so the sign of the $(p_K + p_{\pi})_{\mu}$ coefficient in (25a) is positive. On the other hand, the effective long-distance current can be expressed as

$$j_{\mu,LD}^{\text{eff}} \propto \langle \pi^0 | H_w | K_L \rangle (p_K + p_{\pi})_{\mu}$$

and $\langle \pi^0 | H_w | K_L \rangle$ is negative (given the analysis of Ref. 4) for the same KM matrix convention as in Ref. 21. Thus the long- and short-distance contributions to $K_{\pi e \bar{e}}$ interface destructively to

$$|A| = (2.8 \pm 1.3) \times 10^{-9} m_K^{-2}. \quad (27)$$

Given the possible reduction in the charge-radii difference in (23) by up to a factor of 2 and the larger error on (27), the agreement with observation (21) appears to be reasonable. We might even say that the short-distance scale (26) pins down the long-distance amplitude (24) and therefore (27) to near the lower error, $|A| \sim 1.8 \times 10^{-9} m_K^{-2}$, which is then close to experiment.

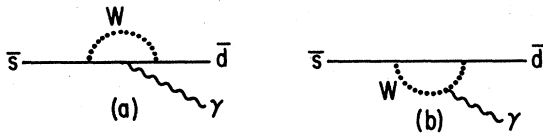


FIG. 8. Short-distance radiative s - d -quark diagram contributing to $K^+ \rightarrow \pi^+ e \bar{e}$ decay.

Although we do not include QCD corrections here, we note that our short-distance estimate (26) is not incompatible with Ref. 15, whose C_7 coefficient $\ln m_c^2/\mu^2$ should be evaluated at $\mu \sim 1$ GeV for $n_f = 3$, where³³ $\Lambda_{\overline{\text{MS}}}(3) \approx 250$ MeV ($\overline{\text{MS}}$ denotes modified minimal-subtraction scheme) for $\alpha_s(\mu^2) \approx 0.5$, corresponding to $\Lambda_{\overline{\text{MS}}}(5) \approx 130$ MeV as is now found from QCD phenomenology. Then one has

$$C_7 = (2/9\pi) \ln m_c^2/\mu^2 \sim 0.06,$$

which yields 20% of the experimental scale, as does (26). Note, however, that QCD corrections could invalidate our arguments about the relative signs.

There are no long-distance contributions to either $K_S^0 \rightarrow \pi^0 e^+ e^-$ by virtue of $\langle \pi^0 | H_w | K_S \rangle = 0$ up to CP violation, or to $K^+ \rightarrow \pi^+ \nu \bar{\nu}$ since the Z^0 mass is much larger than the momentum transfer involved. These decays are then pure short-distance processes. Note also that $K_L^0 \not\rightarrow \pi^0 e^+ e^-$ if CP is conserved as long as a single photon is exchanged.¹⁵

C. $K \rightarrow \pi \pi \gamma$

Since both $K_S \rightarrow \pi^+ \pi^- \gamma$ and $K^+ \rightarrow \pi^+ \pi^0 \gamma$ have now been measured,¹⁹ we can form the decay rate ratio,

$$\left. \frac{\Gamma_{K_S \rightarrow \pi^+ \pi^- \gamma}}{\Gamma_{K^+ \rightarrow \pi^+ \pi^0 \gamma}} \right|_{\text{expt}} \approx 930, \quad (28a)$$

which displays the striking $\Delta I = \frac{1}{2}$ enhancement analogous to

$$\left. \frac{\Gamma_{K_S \rightarrow \pi^+ \pi^-}}{\Gamma_{K^+ \rightarrow \pi^+ \pi^0}} \right|_{\text{expt}} \approx 450. \quad (28b)$$

Alternatively we may examine the branching ratios

$$B(K_S \rightarrow \pi^+ \pi^- \gamma / \pi^+ \pi^-)_{\text{expt}} \approx 0.0027, \quad (28c)$$

$$B(K^+ \rightarrow \pi^+ \pi^0 \gamma / \pi^+ \pi^0)_{\text{expt}} \approx 0.0013,$$

both of which are suppressed by the typical bremsstrahlung scale factor of $\alpha/\pi \sim 0.0023$. These results argue

convincingly for the dominance of the long-distance hadronic-bremsstrahlung graphs and for the continuation of the $\Delta I = \frac{1}{2}$ rule via the amplitudes

$$M_{K_S \rightarrow \pi^+ \pi^- \gamma}^{\text{LD}} = e M_{K_S \pi^+ \pi^-} \left[\frac{p_{\pi^+}}{p_{\pi^+} \cdot k} + \frac{p_{\pi^-}}{p_{\pi^-} \cdot k} \right] \cdot \epsilon^*(k), \quad (29a)$$

$$M_{K^+ \rightarrow \pi^+ \pi^0 \gamma}^{\text{LD}} = e M_{K^+ \pi^+ \pi^0} \left[\frac{p_{\pi^+}}{p_{\pi^+} \cdot k} - \frac{p_{K^+}}{p_{K^+} \cdot k} \right] \cdot \epsilon^*(k). \quad (29b)$$

The factor-of-2 difference between (28a) and (28b) or in (28c) could then be due to the kinematical variation in (29a) and (29b), or to smaller $s \rightarrow d\gamma$ contributions ($\sim 20\%$ or less) as in $K \rightarrow \pi e \bar{e}$ or due to both effects.

We follow Ref. 16, which argues that the $s \rightarrow d\gamma$ short-distance contribution is small and integrates over (29a) for $\omega_\gamma > 50$ MeV to find [calling (29a) the IB contribution]

$$\Gamma_{K_S \rightarrow \pi^+ \pi^- \gamma}^{\text{IB}} = 0.00255 \Gamma_{K_S \rightarrow \pi^+ \pi^-}. \quad (30)$$

Since (30) is so close to (28c), we may presume that (29a) is essentially the entire $K_S \rightarrow \pi^+ \pi^- \gamma$ amplitude. We only differ from Ref. 16 in interpreting (29a) as a long-distance contribution driven directly by $\langle \pi | H_w | K \rangle$ in (1)–(3).

V. SUMMARY

We have first shown that $K_{2\pi}$ and $K_{3\pi}$ decays self-consistently require the same $\Delta I = \frac{1}{2}$ scale of

$$|\langle \pi^0 | H_w | K_L \rangle| \simeq 3.9 \times 10^{-8} \text{ GeV}^2,$$

which is one-half the value found in the original references on this work based on the naive “chain rule”^{2,26}

$$|\langle n\pi^0 | H_w | K^0 \rangle| \simeq (2f_\pi)^{-1} |\langle (n-1)\pi^0 | H_w | K^0 \rangle|.$$

This $\Delta I = \frac{1}{2}$ scale then uniformly predicts dominant long-distance contributions to the other observed kaon decays: $K_{L\gamma\gamma}$, $K_{L\mu\bar{\mu}}$, $K_{\pi^+ e \bar{e}}$, $K_{2\pi\gamma}^0$. We have also estimated the short-distance quark contributions to the latter four decays and find them typically $\sim 20\%$ of the associated long-distance contributions and of the opposite sign.

Note added in proof. While the theoretical estimate in Ref. 4 of $\langle 0 | H_w | K^0 \rangle$ is somewhat unclear, a more recent treatment of $\langle \pi^0 | H_w | K_L \rangle$ for the s - d quark self-energy graph with W exchange based on light-plane wave functions obtains a $\Delta I = \frac{1}{2}$ scale of $-3.4 \times 10^{-8} \text{ GeV}^2$, consistent with the phenomenological findings of this study [N. Fuchs and M. Scadron, University of Arizona report, 1985 (unpublished)].

ACKNOWLEDGMENTS

G. E. thanks the University of Arizona for hospitality; M. D. S. acknowledges support from the U.S. Department of Energy under Contract No. DE-AC02-80ER10663.

*Permanent address: Physics Department, Technion, Haifa, Israel.

¹M. A. Shifman, A. I. Vainshtein, and V. I. Zakharov, Zh. Eksp. Teor. Fiz. **22**, 123 (1975) [JETP Lett. **22**, 55 (1975)]; Nucl. Phys. **B120**, 316 (1977).

²For a review of the original literature, see R. E. Marshak, Riazuddin, and C. P. Ryan, *Theory of Weak Interactions in Particle Physics* (Academic, New York, 1969); D. Bailin, *Weak Interactions* (Sussex University Press, U.K., 1977).

³For a recent review, see M. D. Scadron, Rep. Prog. Phys. **44**, 213 (1981).

⁴B. H. J. McKeller and M. D. Scadron, Phys. Rev. D **27**, 157 (1983). See note added in proof.

⁵N. Cabibbo, Phys. Rev. Lett. **10**, 531 (1963); S. Glashow, J. Iliopoulos, and L. Maiani, Phys. Rev. D **2**, 1285 (1970).

⁶H. F. Jones and M. D. Scadron, Nucl. Phys. **B155**, 409 (1979); H. Genz, Acta Phys. Austriaca Suppl. **21**, 559 (1979); M. D. Scadron, Phys. Rev. D **29**, 2076 (1984).

⁷A. DeRújula, H. Georgi, and S. Glashow, Phys. Rev. D **12**, 147 (1975); N. Isgur, *ibid.* **12**, 3770 (1975).

⁸M. Kobayashi and T. Maskawa, Prog. Theor. Phys. **49**, 652 (1973).

⁹See, e.g., M. W. Reay, invited talk at *International Symposium on Lepton and Photon Interactions at High Energies, Ithaca, New York*, edited by D. G. Cassel and D. L. Kreinick (Newman Laboratory of Nuclear Studies, Cornell University, Ithaca, 1983), and references therein.

¹⁰F. Inami and C. S. Lim, Prog. Theor. Phys. **65**, 297 (1981).

¹¹N. G. Deshpande and G. Eilam, Phys. Rev. D **26**, 2463 (1982).

¹²G. Eilam and M. D. Scadron, University of Arizona report (in

preparation).

¹³E. Ma and A. Pramudita, Phys. Rev. D **24**, 2476 (1981).

¹⁴C. G. Callan and S. B. Treiman, Phys. Rev. Lett. **16**, 197 (1966); Y. Hara and Y. Nambu, *ibid.* **16**, 875 (1966).

¹⁵F. J. Gilman and M. B. Wise, Phys. Rev. D **21**, 3150 (1980).

¹⁶J. L. Lucio, Phys. Rev. D **24**, 2457 (1981).

¹⁷S. Weinberg, Phys. Rev. Lett. **17**, 616 (1966); H. Osborn, Nucl. Phys. **B15**, 501 (1970).

¹⁸J. Cronin, Phys. Rev. **161**, 1483 (1967).

¹⁹Particle Data Group, M. Roos *et al.*, Phys. Lett. **111B**, 1 (1982).

²⁰R. Delbourgo and M. D. Scadron, Phys. Rev. D **28**, 2345 (1983); M. D. Scadron, Z. Phys. C **23**, 237 (1984).

²¹We follow the KM phase conventions as in F. J. Gilman and M. B. Wise, Phys. Lett. **83B**, 83 (1979).

²²S. L. Adler, Phys. Rev. **177**, 2426 (1979); J. S. Bell and R. Jackiw, Nuovo Cimento **60**, 47 (1969).

²³This relative sign follows independently by directly computing the quark tadpole graph or by comparing the $\Delta I = \frac{1}{2} \langle \pi | H_w | K \rangle$ in $K_{2\pi}^0$ decays with the $\Delta I = \frac{3}{2}$ vacuum-saturated transition which occurs at the 5% level in $K_{2\pi}^0$ decays, but dominates $K_{2\pi}^+$ decay.

²⁴L. M. Sehgal, Nuovo Cimento **45**, 785 (1966).

²⁵L. Ametller, L. Bergström, A. Bramon, and E. Massó, Nucl. Phys. **B228**, 301 (1983); M. D. Scadron and M. Visinescu, Phys. Rev. D **29**, 911 (1984).

²⁶M. K. Gaillard and B. W. Lee, Phys. Rev. D **10**, 897 (1974).

²⁷L. Bergström, E. Massó, P. Singer, and D. Wyler, CERN report, 1983 (unpublished).

²⁸C. Hill and G. C. Ross, Phys. Lett. **94B**, 234 (1980); M. B.

- Gavela, A. Le Yaouanc, L. Oliver, O. Pène, and J. C. Raynal, Phys. Lett. **148B**, 248 (1984); J. F. Donoghue, Phys. Rev. D **30**, 1499 (1984); T. N. Pham, Ecole Polytechnique Report No. A606.0584, 1984 (unpublished).
- ²⁹We choose Condon and Shortley phase conventions here. Such sign phases have been a problem in $D_{K\pi}$ decays; see G. Eilam, M. D. Scadron, and B. H. J. McKellar, University of Arizona report, 1983 (unpublished); M. D. Scadron, Phys. Rev. D **29**, 1375 (1984).
- ³⁰L. Ametller, C. Ayala, and A. Bramon, Phys. Rev. D **24**, 233 (1981).
- ³¹A. I. Vainshtein, V. I. Zakharov, L. B. Okun, and M. A. Shifman, Yad. Fiz. **24**, 820 (1976) [Sov. J. Nucl. Phys. **24**, 427 (1976)]. We disagree with their (non- $\Delta I = \frac{1}{2}$) vacuum-saturated estimate of $\langle \pi^+ | H_w | K^+ \rangle$ in Eq. (21).
- ³²R. Tarrach, Z. Phys. C **2**, 221 (1979); S. B. Gerasimov, Yad. Fiz. **29**, 513 (1979) [Sov. J. Nucl. Phys. **29**, 259 (1979)].
- ³³R. Miller and B. McKellar, J. Phys. G **7**, L247 (1981); Phys. Rep. **106**, 170 (1984).